GEOPHYSICS, VOL. 68, NO. 4 (JULY-AUGUST 2003); P. 1417–1422, 6 FIGS., 1 TABLE.
10.1190/1.1598135

Estimating the distribution of primary reflection coefficients

Danilo R. Velis*

ABSTRACT

The distribution of primary reflection coefficients can be estimated by means of the maximum entropy method, giving rise to smooth nonparametric functions which are consistent with the data. Instead of using classical moments (e.g. skewness and kurtosis) to constraint the maximization, nonconventional sample statistics help to improve the quality of the estimates. Results using real log data from various wells located in the Neuquen Basin (Argentina) show the effectiveness of the method to estimate both robust and consistent distributions that may be used to simulate realistic sequences.

INTRODUCTION

Estimating the probability density function (pdf) of primary reflection coefficients is important for the testing and development of new seismic processing algorithms. A realistic quantitative understanding of the underlying process would be useful for deepening our knowledge about the nature of the statistical properties of seismic reflection sequences, and for enhancing the reliability and accuracy of deconvolution operators (Saggaf and Robinson, 2000).

Some authors in the geophysical community focus on estimating the pdf by fitting the sample data to a predefined model (Painter et al., 1995; Walden and Hosken, 1986). These strategies belong to the class of parametric methods, because a finite set of control parameters are fitted to the data. The method of moments and the maximum likelihood (ML) method, for example, belong to this group. Sometimes, a predefined pdf poorly describes a complicated physical phenomenon such as the deposition of sedimentary layers and lithologic units through time. Alternatively, nonparametric methods do not assume any pdf form. The histogram, perhaps the simplest method of this group, has been used as an auxiliary tool in the analysis of the distribution and spectral properties of seismic log data (Todoeschuck et al., 1990; Painter et al., 1995; Jones and Holliger, 1997). As is well known, the histogram presents some drawbacks: the results depend on the bin size and the origin of the bins. In addition, the resulting pdf might not be smooth, especially for short sequences.

The purpose of this work is to emphasize that for further studies of seismic log data, alternative nonparametric methods that produce smooth pdfs are important. Also, it is emphasized that the use of nonconventional statistics which measure distribution shape give results which are more robust and consistent than those using standard measures such as conventional skewness and kurtosis (Ulrych et al., 2000; Velis, 2000). In particular, L-moments and certain skewness and kurtosis indices (which I call S-measures) are combined with the maximum entropy (MaxEnt) method (Jaynes, 1957; Gouveia et al., 1996) to obtain the least informative pdf which is consistent with the available information. That is, we start off with no reason to prefer any pdf over any other and, being as conservative as possible, we pick the one that satisfies some constraints. Whether or not the underlying process corresponds to a specific family of known pdfs (e.g., a generalized Gaussian or a mixture of Laplace distributions) is beyond the scope of this work.

SHAPE INDICES

Quantifying the shape of a distribution is important in data analysis. Reservoir and sedimentary rock characterization, well log studies, and various related modeling, inversion, and processing techniques constitute a few examples of earth sciences applications where quantifying the statistical properties of the media is important. In this context, the shape of the distribution of the process at hand, plays a central role for further investigations as well as in the testing and designing of new processing algorithms (e.g., Walden, 1993; Lancaster and Whitcombe, 2000; Saggaf and Robinson, 2000).

Classical skewness and kurtosis are two of the main indices that characterize shape and are included in most commercial statistical packages. Skewness is associated with symmetry (or lack of symmetry), and kurtosis is usually associated with tail heaviness, pdf peakedness, bimodality, or any combination of the three concepts. Classical skewness and kurtosis are higher order moments which are difficult to estimate when sample size is small because they are too sensitive to moderate

Manuscript received by the Editor October 25, 2001; revised manuscript received November 27, 2002.
*Facultad de Ciencias Astronómicas y Geofísicas, Universidad Nacional de La Plata, Paseo del Bosque s/n, (B1900FWA) La Plata, Argentina. E-mail: velis@fcaglp.unlp.edu.ar.

fluctuations in the tail of the distribution (where outliers may be present). This is the main motivation for developing new skewness and kurtosis measures, such as L-moments and S-measures, which are more robust, less biased, and more consistent for small (say $n < 1000$) sample sizes (Hosking, 1990; Seier, 1998; Ulrych et al., 2000). As in the case of conventional moments, L-moments, which are linear combination of order statistics, are defined for increasing orders. S-measures are shape indices devised to measure skewness and kurtosis only.

In a practical context, given the sequence of primary reflection coefficients $\{r_1, \ldots, r_n\}$ with mean $\bar{r}$ and variance $\bar{s}^2$, conventional normalized skewness and kurtosis (third- and fourth-order moments) are estimated using average values:

$$\sqrt{\beta_1} = \frac{1}{n}\sum_{i=1}^{n}\frac{(r_i-\bar{r})^3}{\bar{s}^3} \quad \text{and} \quad \beta_2 = \frac{1}{n}\sum_{i=1}^{n}\frac{(r_i-\bar{r})^4}{\bar{s}^4}. \quad (1)$$

Hosking (1990) has shown that the first four L-moments are $\ell_1 = \gamma_0$, $\ell_2 = 2\gamma_1 - \gamma_0$, $\ell_3 = 6\gamma_2 - 5\gamma_1 + \gamma_0$, and $\ell_4 = 20\gamma_3 - 30\gamma_2 + 12\gamma_1 - \gamma_0$, respectively, where γ_j may be estimated by means of

$$\hat{\gamma}_j = \frac{1}{n}\sum_{i-1}^{n}\frac{(i-1)(i-2)\cdots(i-j)}{(n-1)(n-2)\cdots(n-j)}r_i, \quad (2)$$

provided the sample has been previously ordered. Akin to the definition of conventional normalized moments,

$$\tau_1 = \frac{\ell_3}{\ell_2} \quad \text{and} \quad \tau_2 = \frac{\ell_4}{\ell_2} \quad (3)$$

are statistics related to the skewness and kurtosis of the pdf, usually called L-skewness and L-kurtosis.

Seier (1998) proposed a family of skewness and kurtosis measures of the form $E[g(f(Z))]$, where $E[\cdot]$ stands for expectation, g is a linear function, f is an odd or even continuous function, and Z is the standardized variable. Some common skewness and kurtosis measures are identified as members of this family, such as $\sqrt{\beta_1} = E[Z^3]$ and $\beta_2 = E[Z^4]$. Two other interesting members, which I call S-skewness and S-kurtosis for convenience, are $\theta_1 = E[a_1 Z|Z|^{b_1}]$ and $\theta_2 = E[a_2 b_2^{-|Z|}]$, respectively. Here a_1, b_1, a_2, and b_2 are constants that I choose to be $a_1 = 2$, $b_1 = 0.5$, $a_2 = 5.7344$, and $b_2 = e$ ($a_2 = 5.7344$ is to honor $\theta_2 = 3$ for a normal distribution).

In practice, θ_1 and θ_2 are estimated using

$$\theta_1 = \frac{2}{n}\sum_{i=1}^{n}\frac{(r_i-\bar{r})|r_i-\bar{r}|^{1/2}}{\bar{s}^{3/2}} \quad \text{and} \quad \theta_2 = \frac{a_2}{n}\sum_{i=1}^{n}e^{-\frac{|r_i-\bar{r}|}{\bar{s}}}. \quad (4)$$

Figure 1 depicts skewness versus kurtosis as estimated using equations (1), (3), and (4) for 500 independent samples

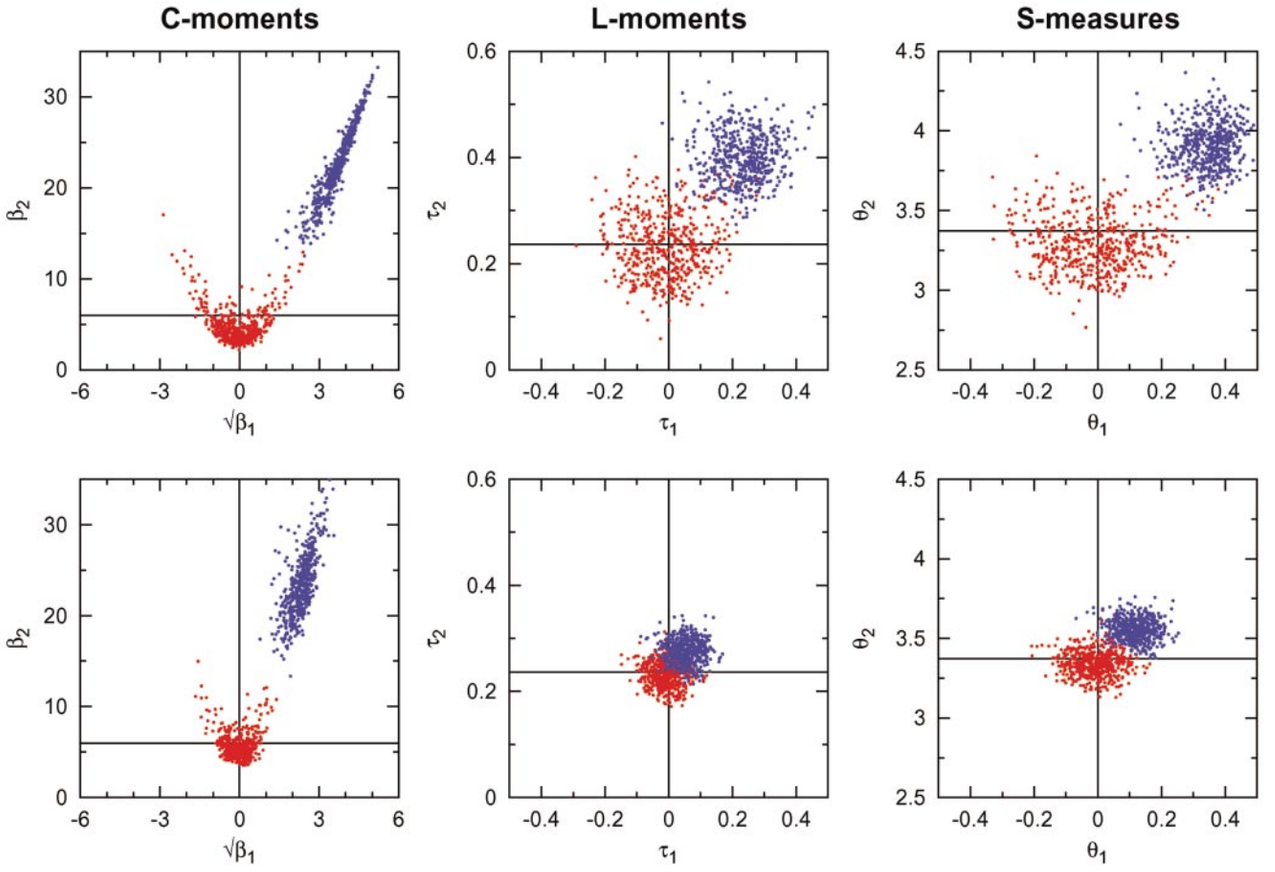

FIG. 1. Estimated skewness ($\sqrt{\beta_1}$) versus kurtosis (β_2), L-skewness (τ_1) versus L-kurtosis (τ_2), and S-skewness (θ_1) versus S-kurtosis (θ_2), corresponding to 500 samples of size $n = 50$ (top row) and $n = 250$ (bottom row). All samples are drawn from a Laplace distribution without outlier (red dots) and with an outlier at 1.75 (blue dots).

($n=50$ and $n=250$) drawn from the Laplace distribution $p(r)=\frac{1}{2\eta}\exp-|r-\mu|/\eta$ with mean $\mu=0.0$ and scale $\eta=8.0$. The high correlation between the conventional moments reveals they are rather correlated measures. As expected, the variability of all the indices decreases with sample size, but not the bias under the presence of an outlier at 1.75. The bias is very high for the C-moments, even for $n=250$. In these simulations, the Laplace distribution has been selected because primary reflection coefficients usually exhibit a Laplace-like distribution (Walden and Hosken, 1986).

MAXIMUM ENTROPY METHOD

Let the actual pdf, $p(r)$, be discretized and represented by the finite sequence $\{p_i\}, i=1,\ldots,m$. Here, it is assumed that p has approximate finite support; that is, $p(r)\simeq 0$ for $r\notin[a,b]$, a and b being the minimum and maximum r of a given sample. A very useful method for conservatively assigning probabilities consists of maximizing the entropy, $H(p)=-\sum_i p_i\log p_i$, subject to constraints on its moments (Jaynes, 1957). The available information is given by the natural constraint $\sum_i p_i=1$, and the k moment constraints $\sum_i h_j(r_i)p_i=\hat{\mu}_j$, $j=1,\ldots,k$, where $h_j(r_i)=r_i^j$ and $\hat{\mu}_j$ is the jth-order moment, which is estimated from the data and introduced into the optimization problem through Lagrange multipliers. By replacing $h_j(r_i)$ by $g(f(r_i))$ for $j=3,4$ only, one can use the same algorithm to set S-skewness and S-kurtosis constraints instead of the classical indices.

The solution of the described constrained optimization problem leads to

$$p_i = e^{-\lambda_0-\sum_{j=1}^{k}\lambda_j h_j(r_i)}, \qquad i=1,\ldots,m \tag{5}$$

where $\lambda_j\,(j=0,\ldots,k)$ are Lagrange multipliers, which are obtained by solving a set of $k+1$ nonlinear equations. These equations come from replacing the solution [equation (5)] into each of the $k+1$ constraints. For $k=1$ and $k=2$, the solutions are the uniform and normal distributions.

L-moments are defined in terms of the cumulative distribution, $P(r)$, rather than in terms of $p(r)$ (Hosking, 1990), because

$$\gamma_j=\int_0^1 r(P)P^j dP=\int_a^b r\,P^j(r)p(r)dr\simeq\sum_i r_i P_i^j p_i. \tag{6}$$

For this reason, constraints using L-moments cannot be easily incorporated into the optimization problem through Lagrange multipliers. Rather, the problem is transformed into an unconstrained optimization problem by defining the cost function

$$J=-H+\alpha\left(\sum_i p_i-1\right)^2+\alpha\sum_j(\ell_j-\hat{\ell}_j)^2, \tag{7}$$

where α is a constant (Ulrych et al., 2000). J is then minimized with respect to the unknown distribution using a multidimensional minimization algorithm.

EXAMPLES

The examples are based on density and sonic logs taken from various wells located in the Neuquen Basin (Estancia Vieja, Río Negro Province, Argentina). The reflectivities corresponding to wells EV11, EV13, and EV17 are shown in Figure 2. The number of measurements (length of the sample vectors) range from 8400 to 11 700, with a sampling depth interval of 0.2 m. Reflection coefficients are calculated, as usual, with $(I_{i+1}-I_i)/(I_{i+1}+I_i)$, where $I_i=\rho_i v_i$ is the impedance at the ith layer with density ρ_i and velocity v_i.

MaxEnt estimates for various sample sizes, using C-moments, L-moments, and S-measures constraints, were computed as described in the previous section. In all cases, I set $m=151$ and $k=4$. In the S-measures case, mean and variance were used as constraints together with θ_1 and θ_2. For

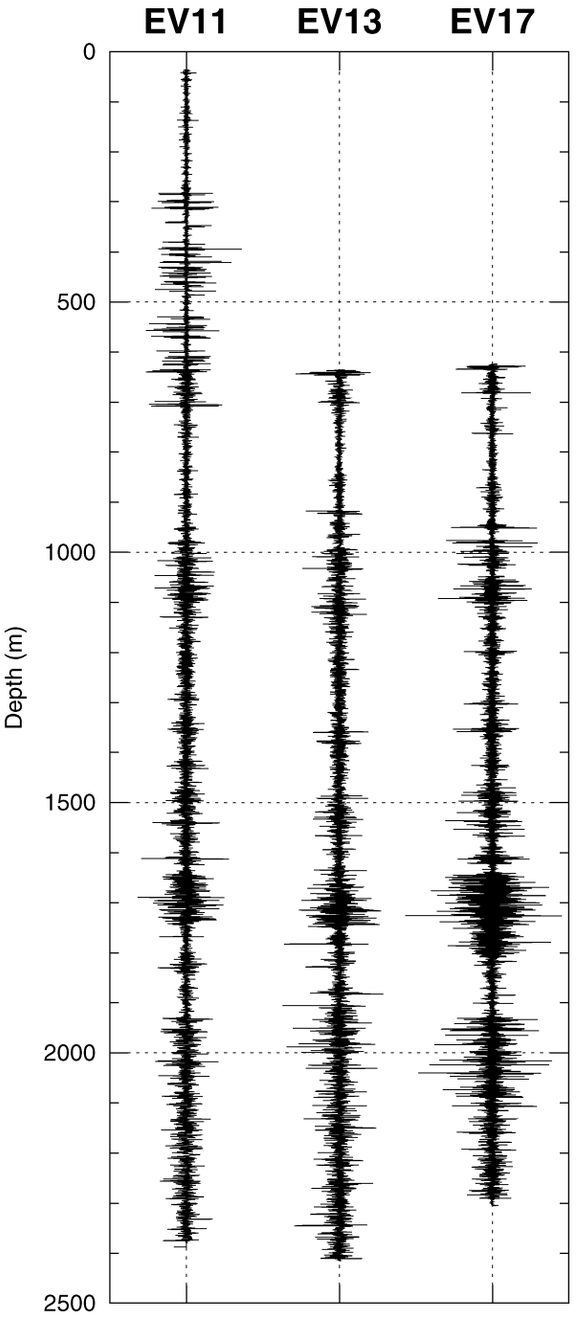

FIG. 2. Reflectivity sequences for wells EV11, EV13, and EV17. Sampling depth interval equals 0.2 m.

comparison, all examples show the pdf derived using a kernel approach, specifically the Epanechnikov kernel (Silverman, 1986), as well as the histogram constructed using centered bins of widths 0.005 (for $n = 100$ and 1000), and 0.0025 (for the complete sample vector). For a meaningful comparison, n values were randomly selected from the complete sample vector.

Results for well EV11 are shown in Figure 3. Assuming that the histogram constructed with $n = 11760$ (complete sample vector) is the closest approximation to the true distribution, it is clear that the central peak of the distribution is best resolved by means of S-measures constraints, even for n as small as 100. Note also that C-moments constraints and, to a lesser extent, L-moments constraints, tend to underestimate the central portion of the pdf. A possible explanation is that higher order C-moments, and in particular classical kurtosis, focus on the tails of the distribution rather than on its peak. This was also observed in synthetic simulations using Laplace pdfs (Ulrych et al., 2000), suggesting that S-measures and L-moments constraints are more appropriate for estimating the pdf of reflection coefficients than C-moments constraints, especially for small values of n. Figure 4 illustrates the results for well EV13. By inspecting the figure, the same conclusions can be drawn for this well as for well EV11. Though not shown, the estimates for other wells exhibit a similar behavior.

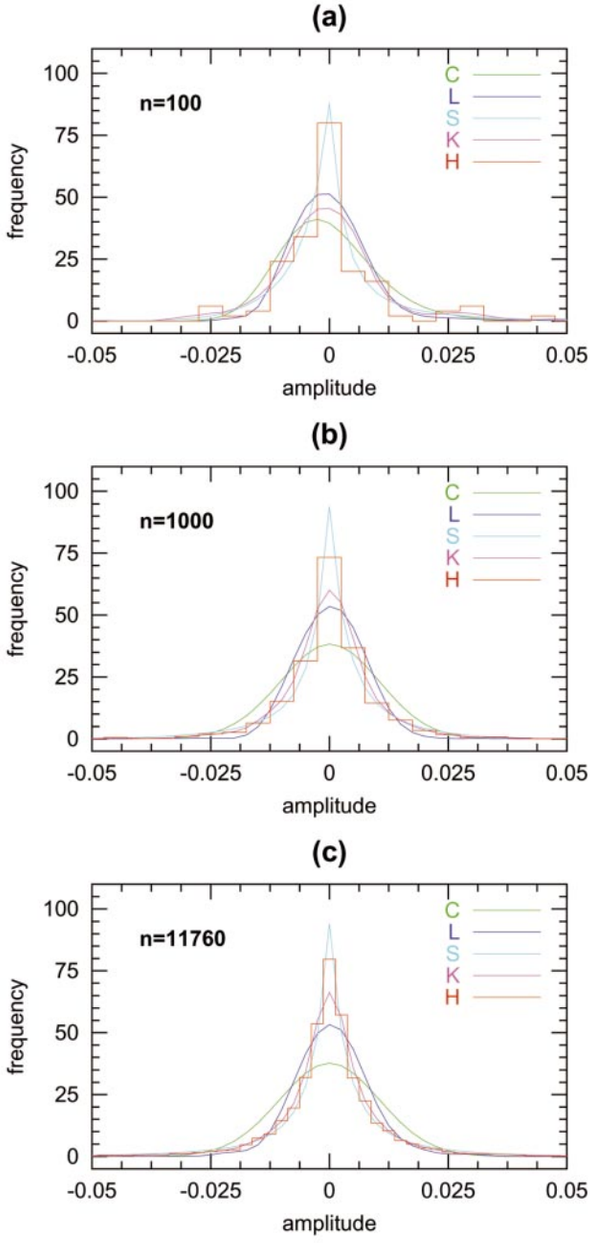

FIG. 3. Pdf estimates from well EV11 using (a) $n = 100$, (b) $n = 1000$, and (c) $n = 11760$ (complete sample vector) measurements. C, L, S, K, and H stand for C-moments, L-moments, S-measures, kernel method, and histogram, respectively. Assuming the histogram in (c) represents the closest approximation to the true distribution, the S-measures–derived pdf appears to be the best estimate, even for n as small as 100.

Clearly, the same pdf cannot represent the complete reflectivity sequence, unless it is purely stationary. Figure 5 shows the estimated pdfs from well EV17 corresponding to eight nonoverlapping windows (n ranging from 500 to 1700) selected so as to avoid nonstationary effects, together with the estimates using the complete sample vector ($n = 8400$). The selected windows are marked in Figure 6. The differences among the pdfs reveal (1) nonstationarity effects and/or (2) sensitivity to short data sequences and outliers. Reducing the consequences of the second issue (by using robust statistical measures) is important for obtaining reliable results. In the example, the L-moments and S-measures derived pdfs appear to show more consistency, analysis window to analysis windows, than the C-moments derived ones. Note that four (out of eight) pdfs are very similar in each of Figures 5b and 5c (windows 3, 8, 4, and 2). On the other hand, this behavior is not observed for the C-moments case.

Finally, Figure 6 illustrates various simulated reflectivities using the MaxEnt estimates from well EV17. Here, the simulated reflectivities were obtained via the rejection method (Press et al., 1992) by concatenating the samples drawn from the eight individual estimates in Figure 5. A more complete strategy for generating realistic reflection sequences can be easily devised by combining these simulated data with the scheme proposed by Walden (1993), who incorporates ARMA (1,1) processes to model the spectral structure of the sequences.

To quantify the closeness between the actual and the simulated distributions, some statistical measures can be computed based on the available data. A commonly used measure is given by the greatest distance, D, between the two cumulative distribution functions [the Kolmogorov-Smirnov (K-S) test]. It turns out that D is too sensitive around the median, but Kuiper's statistic, a variant of the K-S test, is not. Kuiper's statistic (Press et al., 1992) guarantees equal sensitivity at all values of the random variable, and are given by

$$V = D_+ + D_- = \max_{a \le r \le b} [\tilde{P}_n(r) - \hat{P}_n(r)] + \max_{a \le r \le b} [\hat{P}_n(r) - \tilde{P}_n(r)], \quad (8)$$

where $\tilde{P}_n(r)$ and $\hat{P}_n(r)$ are the estimated cumulative distribution functions corresponding to the actual and the simulated samples, respectively. These estimates are easily constructed

using step-functions that rise $1/n$ at each sample value. Table 1 shows V corresponding to the eight windows in Figure 6. The results reveal that V is similar in both the L-moments and S-measures cases for all windows. On the other hand, V is larger by a factor of about two to three in the C-moments case, except for window 5, where all perform well.

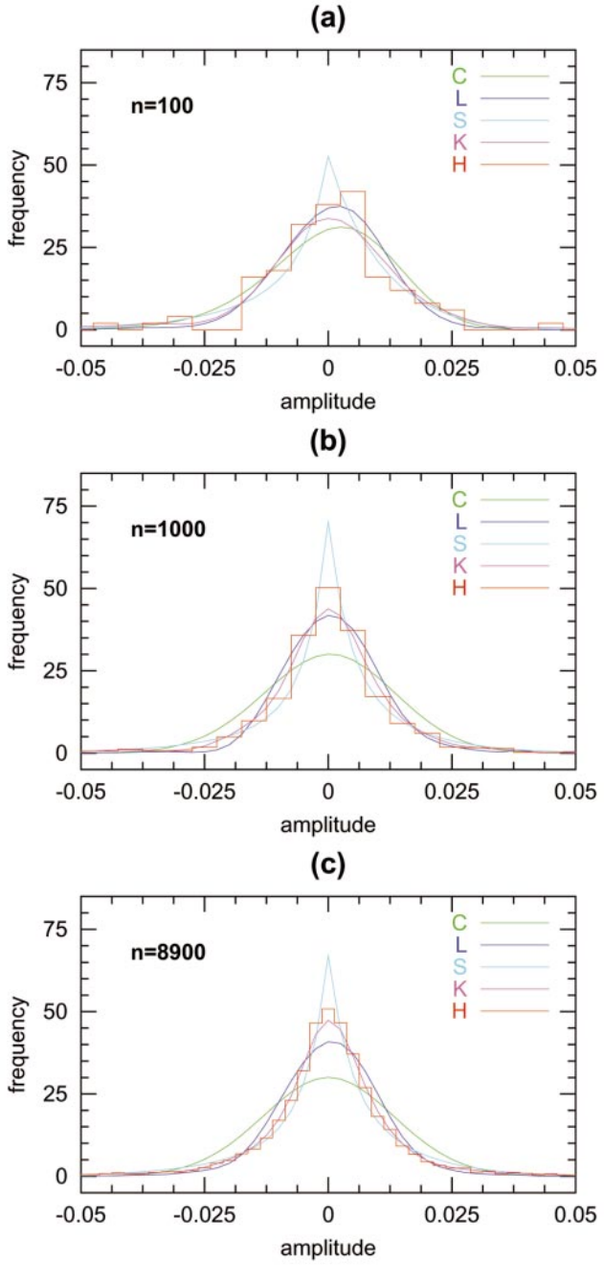

FIG. 4. Pdf estimates from well EV13 using (a) $n = 100$, (b) $n = 1000$, and (c) $n = 8900$ (complete sample vector) measurements. C, L, S, K, and H stand for C-moments, L-moments, S-measures, kernel method, and histogram, respectively. Assuming the histogram in (c) represents the closest approximation to the true distribution, the S-measures derived pdf appears to be the best estimate, even for n as small as 100.

CONCLUSIONS

The derived MaxEnt pdfs are both smooth and consistent with the data. The use of robust nonconventional statistics (L-moments and S-measures) has helped to improve the

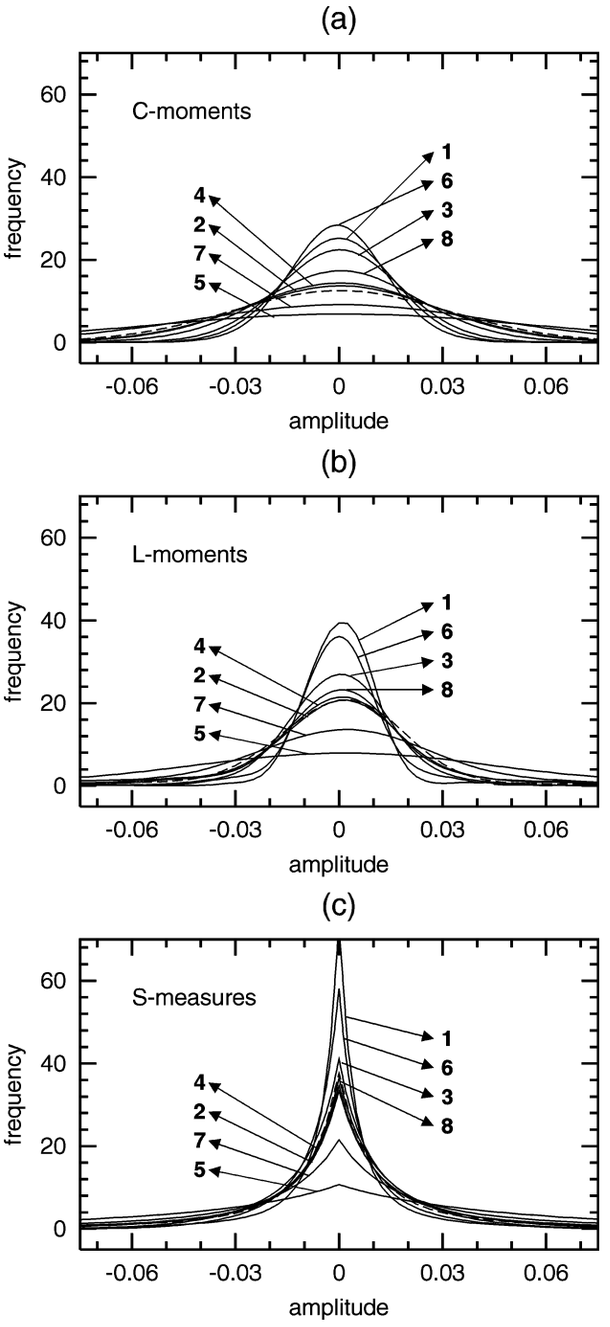

FIG. 5. Pdf estimates from well EV17 (solid line) corresponding to the eight nonoverlapping windows marked in Figure 6 (n ranging from 500 to 1700). (a) C-moments (b) L-moments, and (c) S-measures. The estimates with $n = 8400$ (complete sample vector) are also shown for comparison (dashed line). The L-moments and S-measures derived pdfs appear to show more consistency, analysis window to analysis windows, than the C-moments derived ones. See text for details.

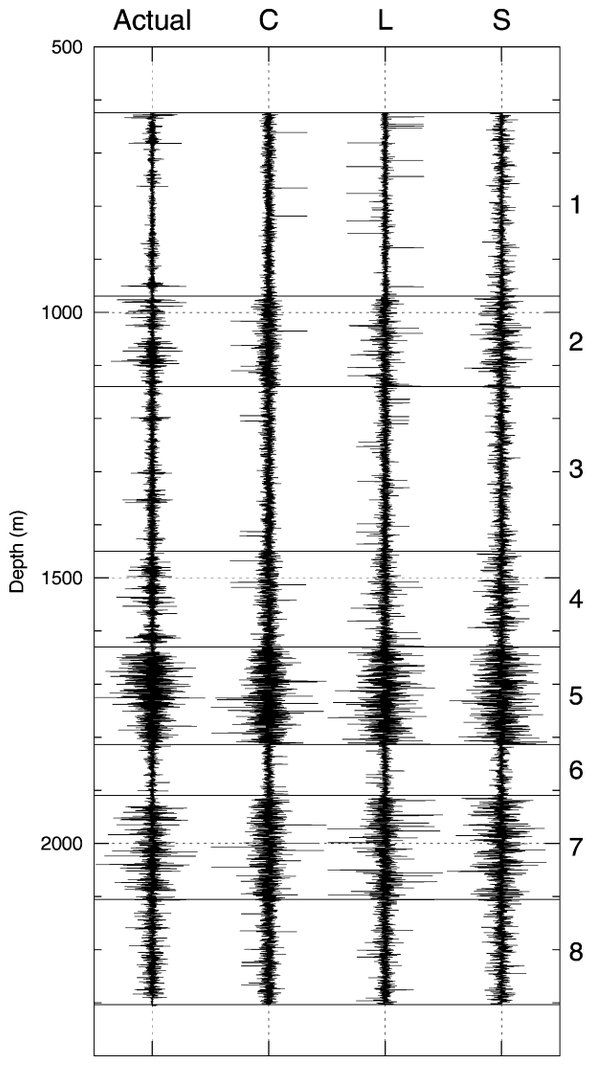

FIG. 6. Actual and simulated reflectivity sequences using the estimates in Figure 5 which correspond to the eight marked nonoverlapping windows (well EV17). Except for window 5, the simulations based on L-moments and S-measures capture best the statistical characteristics of the true sequence, as judged by Kuiper's statistic V shown in Table 1.

accuracy of the results. The obtained pdfs might then be used to analyze the nature of the underlying process, or to define whether the pdf belongs to a certain family of known distributions. Also, the pdf can be used to simulate realistic reflectivity sequences exhibiting the statistical properties of the original data.

Table 1. Kuiper's statistic for the eight windows in well EV17.

Window	C	L	S
1	0.233	0.078	0.071
2	0.174	0.068	0.066
3	0.108	0.060	0.068
4	0.172	0.066	0.070
5	0.088	0.062	0.051
6	0.154	0.076	0.088
7	0.184	0.061	0.067
8	0.133	0.074	0.063

ACKNOWLEDGMENTS

I am grateful to Chevron San Jorge, Argentina, for providing the well log data. I thank James M. Gridley and two anonymous reviewers for their helpful comments and suggestions that contributed to improvement of the manuscript. This work was partially supported by Consejo Nacional de Investigaciones Científicas y Técnicas (PIP 0363/98), Argentina.

REFERENCES

Gouveia, W., Moraes, F., and Scales, J., 1996, Entropy, information and inference, in 1996 CWP Project Review CWP-203: Colorado School of Mines (available at http://www.cwp.mines.edu/).

Hosking, J., 1990, L-moments: analysis and estimation of distributions using linear combinations of order statistics: Internat. J. Roy. Stat. Soc., Ser. B, **52**, 105–124.

Jaynes, E., 1957, Information theory and statistical mechanics: Physical Review, **106**, 620–630.

Jones, A. G., and Holliger, K., 1997, Spectral analyses of the KTB sonic and density logs using robust nonparametric methods: J. Geophys. Res., **102**, 18 391–18 403.

Lancaster, S., and Whitcombe, D., 2000, Fast-track "colored" inversion: 70th Ann. Internat. Mtg., Soc. Expl. Geophys., Expanded Abstracts, 1572–1575.

Painter, S., Beresford, G., and Paterson, L., 1995, On the distribution of seismic reflection coefficients and seismic amplitudes: Geophysics, **60**, 1187–1194.

Press, W. H., Teukolsky, S., Vetterling, W., and Flannery, B., 1992, Numerical recipes *in* FORTRAN: The art of scientific computing, 2nd ed.: Cambridge University Press.

Saggaf, M. M., and Robinson, E. A., 2000, A unified framework for the deconvolution of traces of nonwhite reflectivity: Geophysics, **65**, 1660–1676.

Seier, E., 1998, A family of skewness and kurtosis measures: Ph.D. diss., University of Wyoming.

Silverman, B., 1886, Density estimation for statistics and data analysis: Chapman & Hall.

Todoeschuck, J., Jensen, O., and Labonte, S., 1990, Gaussian scaling noise model of seismic reflection sequences: Evidence from well logs: Geophysics, **55**, 480–484.

Ulrych, T., Velis, D., Woodbury, A., and Sacchi, M., 2000, L-moments and C-moments: Stoch. Envir. Res. and Risk Assessment, **14**, 50–68.

Velis, D. R., 2000, Density estimation using non-conventional statistics: XI Congreso sobre Métodos Numéricos y sus Aplicaciones (XIX ENIEF), Mecánica Computacional, **19**, 359–365.

Walden, A. T., 1993, Simulation of realistic synthetic reflection sequences: Geophys. Prosp., **41**, 313–321.

Walden, A., and Hosken, J., 1986, The nature of the non-Gaussianity of primary reflection coefficients and its significance for deconvolution: Geophys. Prosp., **34**, 1038–1066.